Carbon Nanotubes

International Edition: DOI: 10.1002/anie.201500477
German Edition: DOI: 10.1002/ange.201500477

How a Zigzag Carbon Nanotube Grows**

Qinghong Yuan and Feng Ding**

Abstract: *Owing to the unique structure of zigzag (ZZ) carbon nanotubes (CNTs), their ring-by-ring growth behavior is different from that of chiral or armchair (AC) CNTs, on the rims of which kinks serve as active sites for carbon attachment. Through first-principle calculations, we found that, because of the high energy barrier of initiating a new carbon ring at the rim of a ZZ CNT, the growth rate of a ZZ CNT is proportional to its diameter and significantly (10–1000 times) slower than that of other CNTs. This study successfully explained the broad experimental observation of the lacking of ZZ CNTs in CNT samples and completed the theory of CNT growth.*

The production of single-walled carbon nanotubes (SWCNTs) with any desired atomic structure is crucially important for many applications because each type of SWCNT has its own electronic properties, uniquely depending on its chiral indexes, (n,m). Experimentally, such a goal can be achieved by the post-growth sorting of various SWCNTs samples[1] or by the chirality selective growth of SWCNTs during chemical vapor deposition (CVD) processes as extensively explored experimentally and theoretically.[2] During the sorting of the SWCNTs, two general trends can be clearly seen: 1) the SWCNTs with large chiral angles can be easily sorted and 2) the zigzag SWCNTs with chiral indexes, $(n,0)$, have rarely been sorted. Similar trends have also been seen clearly in the measurements of chirality distributions of various SWCNT samples.[2g–l,3] These experimental results undoubtedly indicates that the growth of SWCNTs is tube structure or chirality dependent.

To understand these experimental puzzles, the theory of screw-dislocation controlled SWCNT growth was proposed.[4] In the theory, a SWCNT with chiral indexes (n,m), where $1 \leq m \leq n$, can be conceptually produced by introducing a m-fold screw dislocation into a $(n,0)$ SWCNT. By applying the classical theory of crystal growth, we can conclude that the rate of atomic attachment to a (n,m) SWCNT is roughly proportional to the number of kinks (or cozy corners) on the SWCNT's rim, m. Therefore the growth rate of a SWCNT should be proportional to m/D or $\sin(\theta)$, where D and θ are the diameter and the chiral angle of the SWCNT, respectively. Such a simple theory was found to fit most experiments very well. It is important to note that, in that theory, the growth rate of ZZ SWCNTs is ignored because of the high formation energy of initiating a new nucleus (i.e., a hexagon) on the smooth rim of a ZZ SWCNT (ca. 1.0 eV[4a]). However, ZZ SWCNTs have been observed despite of their very small amounts.[5] Are the growth rates of ZZ SWCNTs really negligible? And is it possible to synthesize ZZ SWCNTs in large amounts for potential applications? To address these questions is certainly beyond the scope of the previous theory of screw-dislocation-derived SWCNT growth.

Herein, we present a theoretical study on ZZ SWCNT growth from four of the most popular catalysts, Ni, Fe, Co, and Cu. Different from other SWCNTs, the growth of a ZZ SWCNT has a stepwise ring-by-ring behavior and each repeatable step include the nucleation of a new hexagon on the smooth ZZ rim and a subsequent formation of a new hexagon ring. In comparison with the growth of other SWCNTs, where each repeatable step includes the formation of one hexagon only, the growth of ZZ SWCNT is estimated to be 10–1000 times slower. Among the explored catalysts, Fe is recommended for the synthesis of ZZ SWCNTs in large numbers. The study also predicts that the growth of a ZZ SWCNT is inversely proportional to its diameter, or $R \approx 1/D$.

First, let's intuitively discuss the different growth behaviors of ZZ and other SWCNTs. Mimicking the base-growth model, three scenarios of an AC, chiral, and ZZ SWCNTs grow from a catalyst particle surface are shown in Figure 1. The growths of both AC and ZZ SWCNTs occur by the continuous formation of new hexagons on the SWCNT's rim attached to the catalyst particle. These newly formed hexagons on the rim of the AC SWCNT are separated from each other and thus the formation of each is independent. Differently, the firstly formed hexagons on the ZZ SWCNT's rim are the precursor for the formation of following hexagons and thus the formation of these hexagons is not independent. As depicted previously,[4a] the formation of the first hexagon on a ZZ rim leads two AC-like kink sites, which are active for the uptake of C atoms or forming new hexagons. From this simple picture, we can clearly see that a) the growth of an AC SWCNT is a continuous process and each repeatable step of its growth only forms a new hexagon at a AC site (Figure 1a); b) the growth of a chiral SWCNT is similar to that of an AC one because of the existence of AC-like sites on its rim (Figure 1b); c) the growth behavior of a ZZ SWCNT is different and there are two independent steps to form a new

[*] Dr. Q. Yuan
Department of Physics
East China Normal University
Shanghai, 200241 (China)
E-mail: qhyuan@phy.ecnu.edu.cn
Dr. Q. Yuan, Prof. Dr. F. Ding
Institute of Textiles and Clothing
Hong Kong Polytechnic University
Hong Kong (China)
E-mail: feng.ding@polyu.edu.hk

[**] This work was supported by NSFC grant (21303056, 21273189) and Shanghai Pujiang Program (13J1402600), Hong Kong RCF-GRF grant (BQ-26K, B-Q35N, B-Q41N). The computations were performed in the Supercomputer Centre of Tianjin and East China Normal University.

Supporting information for this article is available on the WWW under http://dx.doi.org/10.1002/anie.201500477.

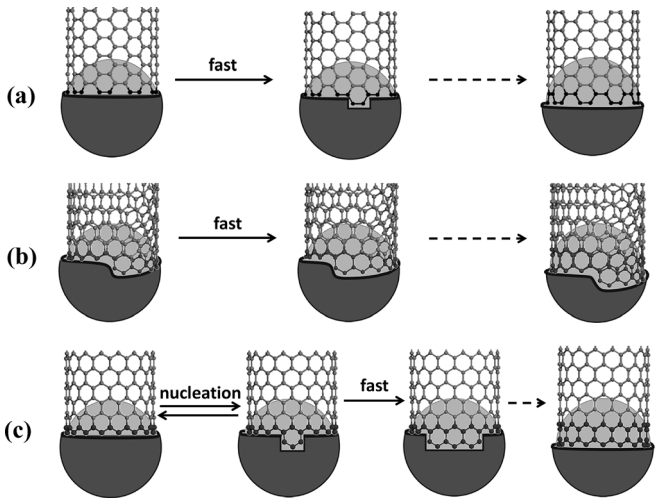

Figure 1. Illustration of the growth behaviors of a) AC, b) chiral, and c) ZZ SWCNTs.

hexagonal ring on its rim, c-i) the nucleation of the first hexagon on its smooth rim and c-ii) the consequent growth of a complete hexagon ring at the rim (Figure 1c).

Based on the above atomistic process of ZZ SWCNT growth, the incorporation of carbon atoms into the ZZ SWCNT zigzag edge are explored. Similar to our previous study of CNT growth by the attachment of C atoms to the AC-like sites,[4a,6] a periodic slab model in which the graphene edge attached to a metal step is used to model a fraction of the interface between the CNT and the catalyst. The generalized gradient approximation (GGA) with Perdew-Burke-Ernzerhof (PBE) functional[7] was used to calculate the energies of incorporating C atoms into the ZZ SWCNT's edge (details see modeling and methods of calculation in Supporting Information).

Starting from a perfect ZZ edge attached to a Ni step, the sequential addition of carbon atoms into the growth front of the ZZ edge until the formation of a complete hexagonal ring is shown in Figure 2b. The formation of the first hexagon involves the incorporation of three carbon atoms in sequence. The formation energies and barriers of incorporating the 1st/2nd/3rd atoms are 1.08/0.78/1.09 and 1.11/2.11/1.03 eV, respectively. After the incorporation of the third atom, a new hexagon is formed and one metal atom is completely knocked out of the interface. As shown in the energy profile (Figure 2a), the overall energy barrier of the first hexagon incorporation is 3.06 eV and the formation of the first hexagon has the energy of 1.26 eV.

The formation of the second hexagon includes the addition of another two C atoms and the removing of another metal atom. The 4th C atom addition is similar to that of the 2nd one and the incorporation of the 5th C atom is similar to that of the 3rd one. The threshold barrier of forming the 2nd hexagon is 2.32 eV (or 3.58 eV if taking the energy of the perfect ZZ edge as reference) and the final structure—the formation of the neighboring hexagon on the ZZ edge has a formation energy of 1.27 eV, which is very similar to the formation energy of the first hexagon, 1.26 eV.

Adding 7, 9, 11 C atoms leads to the formation of three, four, and five neighboring hexagons, respectively, on the ZZ edge. The formation energies of them are 1.10, 1.09, and 1.02 eV, respectively. From here, we can clearly see that the

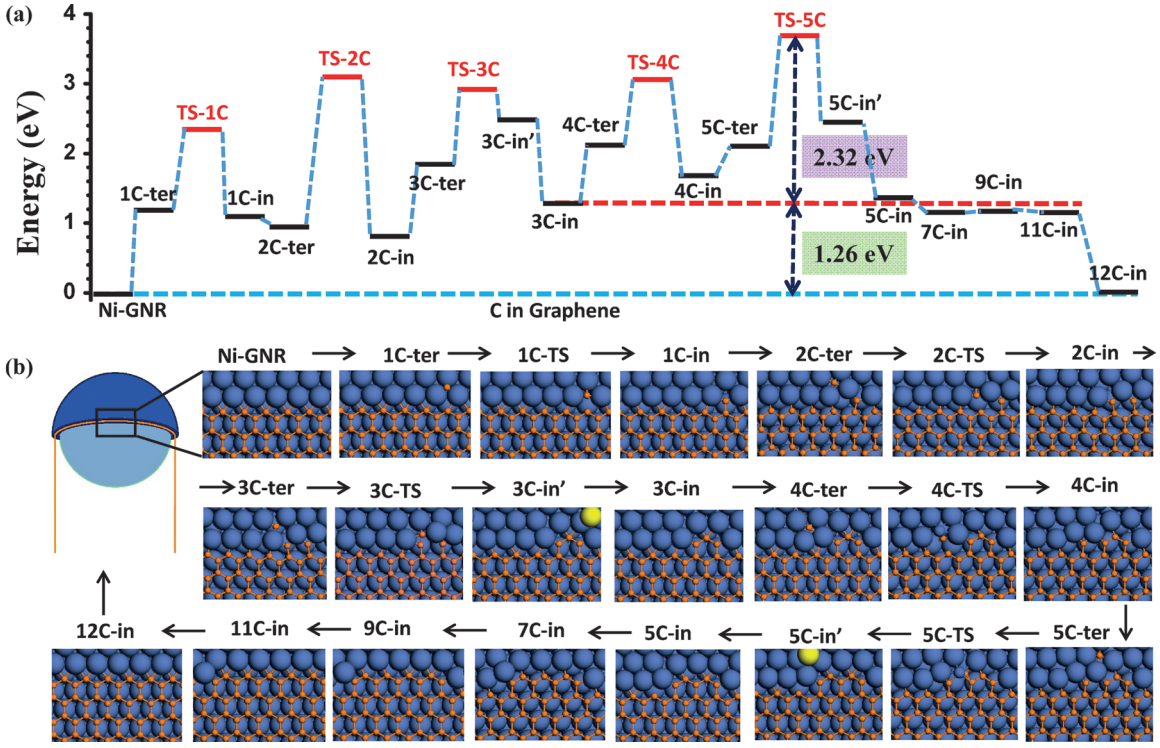

Figure 2. Energy profile (a) and optimized geometries (b) of a complete cycle of zigzag nanotube growth on a Ni catalyst. GNR = graphene nanoribbon, ter = terrace, TS = transition state, in = incorporated carbon with a knocked Ni atom, in′ = incorporated carbon with the knocked Ni atom diffusion to the bulk of Ni, blue = Ni, orange = C, yellow = knocked Ni atom.

formation energies of one to five neighboring hexagons on the rim are very close, which is expected by the kink model shown in previous studies.[4a,8] This result indicates that the formation of the first hexagon drives the system to a high energy state (with two ZZ kinks) and the following sequential addition of each hexagon is repeatable until the whole hexagon row (or hexagon ring on the open end of a ZZ SWCNT) is completed. Different from the previous hexagons, as expected, the formation of the last hexagon, completed by the addition of the last C atom results in a complete hexagon row on the rim and drives the formation energy to 0.0 eV.

It is very important to note that the energy barrier of incorporating a new hexagon near the first one, which is 2.32 eV, is very similar to the overall energy barrier of incorporating a new hexagon to a AC-like site, 2.27 eV.[6] This is expected because the formation of the first hexagon creates two AC-like sites one on each of its shoulders and the formation of the second hexagon exactly corresponds the addition of two C atoms to an AC-like site. Because the overall barrier of the first hexagon on the ZZ edge (3.06 eV) is smaller than that of the second one (3.58 eV), the overall barrier of forming a full hexagon ring on the ZZ SWCNT edge is exactly the formation energy of the first hexagon (E_{ZZ}) plus the energy barrier of forming the second hexagon at the AC-like site (E_{AC}*) [Eq. (1)]:

$$E_{ZZ}{}^{*} = E_{ZZ} + E_{AC}{}^{*} \tag{1}$$

Therefore, the important assumption of the screw dislocation derived SWCNT growth model—that the threshold barrier of ZZ SWCNT growth is the formation energy of a ZZ nucleus plus the barrier of forming a new hexagon on an AC-like site is shown to be valid.

From the above analysis, we can conclude that the formation energy of the first hexagon on the ZZ edge was the crucial parameter that determines the difference between the growth behaviors of ZZ SWCNT and others. To explore the effects of the catalyst, the formation energy of the first hexagon (E_{1f}) on four most used catalysts, Fe, Co, Ni, and Cu, were calculated (Supporting Information, Figure S1). The calculated energies are 0.79, 1.01, 1.26, and 1.26 eV on Fe, Co, Ni, and Cu catalysts, respectively (Figure S1). It can be seen that E_{1f} on the ZZ edge is catalyst-type dependent and Fe has the smallest barrier for ZZ SWCNT growth.

Based on the above understandings on ZZ SWCNT growth and the calculations, it is possible to calculate the growth rate of (n,0) ZZ SWCNTs. A repeatable step of a ZZ SWCNT growth includes two steps—overcoming a barrier of E_{AC}* + E_{ZZ} to stabilize a ZZ nucleus and the subsequent formation of the (n−1) hexagons from both the active sites near the nucleus. According to the transition-state theory, with abundant C atoms around, the time required to stabilize a nucleus can be estimated by Equation (2)

$$\tau_1 = h\beta\frac{\exp\left[\beta\left(E_{AC}^{*} + E_{ZZ}\right)\right]}{n} \tag{2}$$

where h is the Plank constant, $\beta = 1/(kT)$, k is the Boltzmann constant, T is the temperature of SWCNT growth, $n = (\pi D)/$ 0.246 nm is the number of ZZ sites on the edge and D is the diameter of the SWCNT. The time cost to form the following (n−1) hexagons near the vicinity of the nucleus is given by Equation (3)

$$\tau_2 = \frac{(n-1)h\beta\exp\left[\beta E_{AC}^{*}\right]}{2} \tag{3}$$

where the factor 2 corresponds the two active sites of the nucleus on the ZZ SWCNT edge. Thus the growth rate of a ZZ SWCNT can be estimated by Equation (4):

$$R_{ZZ} = \frac{0.213\text{nm}}{\tau_1 + \tau_2} = \frac{n\exp\left(-\beta E_{AC}^{*}\right)0.426\text{nm}}{h\beta[2\exp(\beta E_{ZZ}) + n(n-1)]} \tag{4}$$

where 0.213 nm is the net elongation of the ZZ SWCNT after forming a complete hexagon ring. According to the theory of screw-dislocation-derived SWCNT growth, the growth rate of an AC CNT is given by Equation (5)

$$R_{AC} = \frac{\exp\left(-\beta E_{AC}^{*}\right)0.123\text{nm}}{h\beta} \tag{5}$$

where 0.123 nm is the net elongation of a AC SWCNT after the addition of a complete hexagon ring and $(1/h\beta)\exp[-\beta$-$(E_{AC}$*$)]$ is the average time of forming a new hexagon on the AC rim. So, the ratio of R_{ZZ} to R_{AC} is given by Equation (6):

$$\frac{R_{ZZ}}{R_{AC}} = \frac{3.46n}{2\exp(\beta E_{ZZ}) + n(n-1)} = \frac{10.87D}{0.246\text{nm}\left[2\exp(\beta E_{ZZ}) + \frac{9.86D(D-0.078)}{0.06\text{nm}^2}\right]} \tag{6}$$

Experimentally, typical SWCNTs synthesized have the diameter of approximately 1.0 nm, which corresponds to $n \approx 10$. At a typical temperature of SWCNT growth (e.g., $T \approx$ 800–1300 K), $\beta \approx 10\ \text{eV}^{-1}$. In Equation (4), the ratio of τ_1 to τ_2 can be roughly estimated by Equation (7).

$$\frac{\tau_1}{\tau_2} = \frac{2\exp(\beta E_{ZZ})}{n(n-1)} \tag{7}$$

For typical CVD growth with Fe, Co, or Ni/Cu as the catalyst, τ_1/τ_2 ranges from 25–10^3, 180–10^4, 10^3–10^6, respectively. So, we can conclude that for most CVD experiments, the time of forming subsequent hexagons is negligible in comparison with that for initiating a nucleus on the ZZ rim. Thus the growth rate of a ZZ SWCNT can be estimated by Equation (8).

$$R_{ZZ} \approx \frac{0.213\text{nm}}{\tau_1} = \frac{2.72D\exp\left[-\beta\left(E_{AC}^{*} + E_{ZZ}\right)\right]}{h\beta} \tag{8}$$

Hence, the ratio of R_{ZZ} to R_{AC} becomes [Eq. (9)].

$$\frac{R_{ZZ}}{R_{AC}} \approx \frac{2.72D\exp(-\beta E_{ZZ})}{0.124\text{nm}} \tag{9}$$

The above Equations demonstrated that the growth rate of a ZZ SWCNT is significantly slower than that of AC SWCNTs. For a tube of $D = 1.0$ nm, at the typical

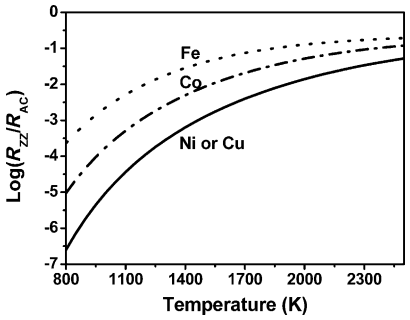

Figure 3. Growth ratio of zigzag SWCNTs with tube diameter of 1 nm and armchair SWCNTs on Ni, Co, Fe, Cu surfaces versus growth temperature.

temperature of tube growth, $\beta \approx 10\ eV^{-1}$, $R_{ZZ}/R_{AC} \approx 10^{-3}$, 10^{-4}, 10^{-5} for Fe, Co, Ni/Cu catalysts, respectively, as shown in Figure 3. The growth rate difference between a $(n,0)$ ZZ SWCNT and a $(n,1)$ SWCNT for $n \approx 10$, is about one order magnitude smaller or $R_{ZZ}/R_{(n,1)} \approx 10^{-2}$, 10^{-3}, and 10^{-4} for these catalysts, respectively. For SWCNTs grown with Fe as the catalyst and at a higher temperature of $T \approx 1300$ K, certainly, noticeable amounts of ZZ SWCNTs could be synthesized.

The effective temperature of SWCNT growth in arc discharge or laser ablation experiments may reaches 2000 °C or higher,[9] which is responsible for the very fast growth of SWCNTs.[6,10] At such a high temperature the growth rate of ZZ tube can be greatly increased because of the great reduction of the time for initiating a nucleus on the ZZ rim, τ_1. As shown in Figure 3, the R_{ZZ}/R_{AC} is increased to 10^{-2}–10^{-1} at a growth temperature of 2500 K. So, it is very possible to find more ZZ SWCNTs in the arc discharge or laser-ablation samples. This is in good agreement with the chirality measurement of arc discharge SWCNT samples, in which SWCNTs of all chiral angles have very similar probabilities of being observed.[5b,c] We further noticed that, in agreement with the prediction, most previously observed ZZ SWCNTs are found in the arc discharge samples.[5b–d]

In addition, Equations (4)–(6) clearly indicate another difference between the growth of ZZ and other SWCNTs is that the growth rate of a ZZ SWCNT is proportional to its diameter. Such a trend originates from the large number of nucleation sites on the edge of a large ZZ SWCNT and is consistent with the nucleation-mediated crystal growth in traditional crystal growth. The predication of linear growth rate versus diameter for ZZ SWCNTs provides a potential route to observe the growth behavior of ZZ SWCNTs experimentally.

In conclusion, we have performed a comprehensive theoretical study on the growth behavior of ZZ SWCNTs, which was predicted to be different from other SWCNTs by the theory of screw-dislocation-derived SWCNT growth. Our analysis and calculations demonstrate that the growth of ZZ CNTs is a stepwise process which involves the nucleation of a hexagon on the ZZ edge and a subsequent formation of a complete hexagon ring. The nucleation of a stable hexagon was found to be the threshold step that limits the growth rate of the ZZ SWCNT. Under the conditions of most chemical-vapor-deposition growth, the growth rate of a ZZ SWCNT is about a few orders magnitudes (10^{-1}–10^{-5}) slower than that of other SWCNT types. Together with other possible reasons that may also contribute to the disadvantage of zigzag CNTs, such as the weak Van der Waals interaction between zigzag CNTs,[11] this study have successfully explained the long standing experimental puzzle of why there is little ZZ CNT in most experimental samples. Our study also shows that the overall barrier of a ZZ SWCNT growth is equal to the sum of formation energy of a stable nucleus (or a hexagon) and the energy barrier of forming a hexagon at an AC-like site, which validated the previously proposed screw-dislocation theory.[4a] We also predict that, among all types of SWCNTs, only the growth of ZZ SWCNTs is diameter dependent and the growth rate increases linearly with its diameter. To achieve the synthesis of ZZ SWCNTs in large number, the use of Fe as catalyst and a high experimental temperature is recommended.

Keywords: carbon nanotubes · chirality · kinetics · nucleation · zigzag carbon nanotubes

How to cite: *Angew. Chem. Int. Ed.* **2015**, *54*, 5924–5928
Angew. Chem. **2015**, *127*, 6022–6026

[1] a) F. Toshimitsu, N. Nakashima, *Nat. Commun.* **2014**, *5*, 5041; b) S. Ghosh, S. M. Bachilo, R. B. Weisman, *Nat. Nanotechnol.* **2010**, *5*, 443–450; c) X. Tu, S. Manohar, A. Jagota, M. Zheng, *Nature* **2009**, *460*, 250–253; d) H. Liu, D. Nishide, T. Tanaka, H. Kataura, *Nat. Commun.* **2011**, *2*, 309.

[2] a) J. Kim, S. Irle, K. Morokuma, *Phys. Rev. Lett.* **2011**, *107*, 175505; b) E. C. Neyts, K. Ostrikov, Z. J. Han, S. Kumar, A. C. T. van Duin, A. Bogaerts, *Phys. Rev. Lett.* **2013**, *110*, 065501; c) E. S. Penev, V. I. Artyukhov, B. I. Yakobson, *ACS Nano* **2014**, *8*, 1899–1906; d) V. I. Artyukhov, E. S. Penev, B. I. Yakobson, *Nat. Commun.* **2014**, *5*, 4892; e) J. Kim, A. J. Page, S. Irle, K. Morokuma, *J. Am. Chem. Soc.* **2012**, *134*, 9311–9319; f) M. F. C. Fiawoo, A. M. Bonnot, H. Amara, C. Bichara, J. Thibault-Penisson, A. Loiseau, *Phys. Rev. Lett.* **2012**, *108*, 195503; g) H. Wang, B. Wang, X.-Y. Quek, L. Wei, J. Zhao, L.-J. Li, M. B. Chan-Park, Y. Yang, Y. Chen, *J. Am. Chem. Soc.* **2010**, *132*, 16747–16749; h) F. Yang, X. Wang, D. Zhang, J. Yang, D. Luo, Z. Xu, J. Wei, J.-Q. Wang, Z. Xu, F. Peng, X. Li, R. Li, Y. Li, M. Li, X. Bai, F. Ding, Y. Li, *Nature* **2014**, *510*, 522–524; i) M. He, A. I. Chernov, P. V. Fedotov, E. D. Obraztsova, J. Sainio, E. Rikkinen, H. Jiang, Z. Zhu, Y. Tian, E. I. Kauppinen, M. Niemelae, A. O. I. Krauset, *J. Am. Chem. Soc.* **2010**, *132*, 13994–13996; j) A. R. Harutyunyan, G. Chen, T. M. Paronyan, E. M. Pigos, O. A. Kuznetsov, K. Hewaparakrama, S. M. Kim, D. Zakharov, E. A. Stach, G. U. Sumanasekera, *Science* **2009**, *326*, 116–120; k) X. Li, X. Tu, S. Zaric, K. Welsher, W. S. Seo, W. Zhao, H. Dai, *J. Am. Chem. Soc.* **2007**, *129*, 15770–15771; l) W.-H. Chiang, R. M. Sankaran, *Nat. Mater.* **2009**, *8*, 882–886.

[3] a) R. Rao, D. Liptak, T. Cherukuri, B. I. Yakobson, B. Maruyama, *Nat. Mater.* **2012**, *11*, 213–216; b) S. M. Bachilo, M. S. Strano, C. Kittrell, R. H. Hauge, R. E. Smalley, R. B. Weisman, *Science* **2002**, *298*, 2361–2366; c) S. M. Bachilo, L. Balzano, J. E. Herrera, F. Pompeo, D. E. Resasco, R. B. Weisman, *J. Am. Chem. Soc.* **2003**, *125*, 11186–11187; d) Y. Sato, K. Yanagi, Y. Miyata, K. Suenaga, H. Kataura, S. Lijima, *Nano Lett.* **2008**, *8*, 3151–3154; e) M. Fouquet, B. C. Bayer, S. Esconjauregui, R. Blume, J. H. Warner, S. Hofmann, R. Schlogl, C. Thomsen, J. Robertson, *Phys. Rev. B* **2012**, *85*, 235411.

[4] a) F. Ding, A. R. Harutyunyan, B. I. Yakobson, *Proc. Natl. Acad. Sci. USA* **2009**, *106*, 2506 – 2509; b) H. Dumlich, S. Reich, *Phys. Rev. B* **2010**, *82*, 085421.
[5] a) H. Telg, J. Maultzsch, S. Reich, F. Hennrich, C. Thomsen, *Phys. Rev. Lett.* **2004**, *93*, 177401; b) K. Hirahara, M. Kociak, S. Bandow, T. Nakahira, K. Itoh, Y. Saito, S. Iijima, *Phys. Rev. B* **2006**, *73*, 195420; c) Z. Liu, Q. Zhang, L.-C. Qin, *Phys. Rev. B* **2005**, *71*, 245413; d) S. S. Wijeratne, N. C. Harris, C.-H. Kiang, *Materials* **2010**, *3*, 2725 – 2734; e) M. Fouquet, B. Bayer, S. Esconjauregui, R. Blume, J. Warner, S. Hofmann, R. Schlögl, C. Thomsen, J. Robertson, *Phys. Rev. B* **2012**, *85*, 235411.
[6] Q. H. Yuan, H. Hu, F. Ding, *Phys. Rev. Lett.* **2011**, *107*, 156101.
[7] J. P. Perdew, K. Burke, M. Ernzerhof, *Phys. Rev. Lett.* **1996**, *77*, 3865 – 3868.
[8] T. Ma, W. C. Ren, X. Y. Zhang, Z. B. Liu, Y. Gao, L. C. Yin, X. L. Ma, F. Ding, H. M. Cheng, *Proc. Natl. Acad. Sci. USA* **2013**, *110*, 20386 – 20391.
[9] a) A. Puretzky, H. Schittenhelm, X. Fan, M. Lance, L. Allard, D. Geohegan, *Phys. Rev. B* **2002**, *65*, 245425; b) C. D. Scott, S. Arepalli, P. Nikolaev, R. E. Smalley, *Appl. Phys. A* **2001**, *72*, 573 – 580; c) Z. Liu, D. J. Styers-Barnett, A. A. Puretzky, C. M. Rouleau, D. Yuan, I. N. Ivanov, K. Xiao, J. Liu, D. B. Geohegan, *Appl. Phys. A* **2008**, *93*, 987 – 993.
[10] Q. H. Yuan, Z. P. Xu, B. I. Yakobson, F. Ding, *Phys. Rev. Lett.* **2012**, *108*, 245505.
[11] a) R. F. Rajter, R. Podgornik, V. A. Parsegian, R. H. French, W. Y. Ching, *Phys. Rev. B* **2007**, *76*, 045417; b) A. Popescu, L. M. Woods, I. V. Bondarev, *Phys. Rev. B* **2011**, *83*, 081406.

Received: January 18, 2015
Published online: March 12, 2015

